Optical Measurements
Paper 20

EXPERIMENTAL DATA FROM OPTICAL MEASUREMENT TESTS ON A TRANSONIC TURBINE BLADE CASCADE

P. Safarik

Department of Fluid Mechanics and Thermodynamics
Czech Technical University
16607 Prague, Czech Republic

Experimental Data from Optical Measurement Tests on a Transonic Turbine Blade Cascade

P.Šafařík
Department of Fluid Mechanics and Thermodynamics
Faculty of Mechanical Engineering
Czech Technical University
Prague, Czech Republic

Abstract

This contribution deals with methods and results of aerodynamic research of a transonic turbine blade cascade. Results of optical measurements are presented and interferograms of flow fields have been evaluated and analysed. An occurrence of supersonic compression accompanying transonic expansion on the suction side of the profile is shown and described. Special methodical problems and problems on aerodynamic choking, boundary layer development, and off-design leading edge separation are discussed.

Nomenclature

b	[mm]	chord
C	$[kg/m^3]$	constant of the interferometric system
i	[-]	number of fringe
K	$[kg/m^3]$	Gladstone-Dale constant
L	[m]	wind tunnel width
o	[mm]	width of the cascade throat
t	[mm]	pitch
x	[mm]	chordwise coordinate
y	[mm]	coordinate of the profile
M_1	[-]	inlet Mach number
M_{2is}	[-]	exit isentropic Mach number
p_{is}	[Pa]	isentropic static pressure
p_0	[Pa]	total pressure
β_1	[°]	inlet angle
γ	[°]	stagger angle
κ	[-]	ratio of heat capacities
λ	[m]	wave length of monochromatic light
λ_{is}	[-]	isentropic nondimensional velocity
ρ	$[kg/m^3]$	flow density

ρ_0	[kg / m^3]	total density
$(\rho)_i$	[kg / m^3]	flow density for the i-th fringe
$(\rho)_0$	[kg / m^3]	flow density for the zero-th fringe

1. Introduction

Optical methods have been utilised during the high-speed aerodynamic research in the Institute of Thermomechanics, Academy of Sciences of the Czech Republic for almost thirty years. This period provided us with large experience. Extensive sets of experimental data mostly from interferometric and schlieren measurements have been collected. Our archive contains more than ninety thousand pictures. The aim of this paper is to describe our facility, and to present and discuss some of the results of our aerodynamic research.

2. The Optical Measurement System

The optical measurement system developed in the Institute of Thermomechanics is depicted schematically in Fig. 1. The optical system consists of the light system, the internal system of the Mach-Zehnder type interferometer, and the image system. A mercury lamp is used as a source of light for setting up the whole system. During the experiments a spark generator is used when the mercury lamp light is covered. The spark generator light passes through the interference filter. The coherent light is divided into two branches on the left bottom half-permeable mirror of the interferometer. The measuring light branch passes through the test section and the comparative light branch passes through the compensator. The interferometric image of the flow field in the test section with the blade cascade appears on the top

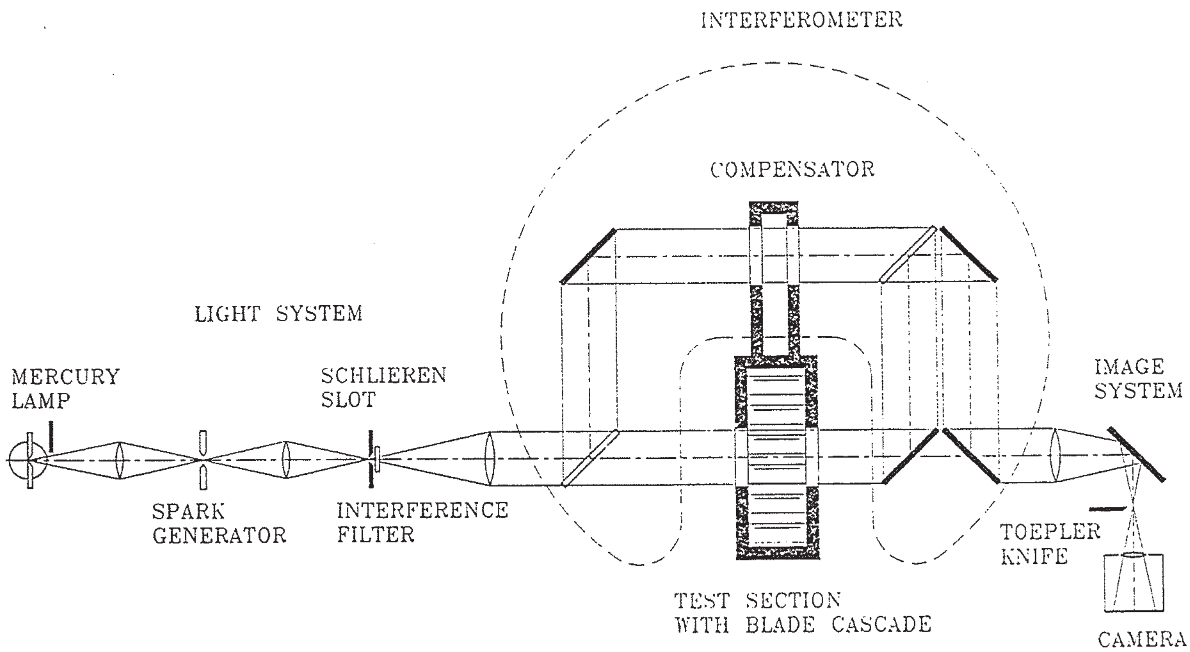

Fig. 1 The scheme of the optical system

right half-permeable mirror. The image is recorded by a camera in the image system. The interferometric arrangement can be easily modified to the schlieren system. The schlieren slot substitutes the interference filter in the light system focus, the comparative light branch is covered, and the Toepler knife is inserted into the image system focus. The briefly described optical device has been applied many times and proved to be very reliable. The neccessity of a very high-precision production of all glass optical parts is a disadvantage of this system. Another disadvantage is the fact that images can be focused only on a limited density region.

3. The SE 1050 Turbine Blade Cascade

Several years ago we made a proposal to use the SE 1050 turbine blade cascade as the etalon cascade. For its detailed description and the test results, see [1] and [2]. The scheme of the cascade is in Fig. 2. The cascade can be found in the rotor blading of the last stage of a ŠKODA steam turbine of large output. Different research techniques can be verified by means of the empirical data obtained on the blade cascade. It has often been utilised by composers of numerical methods.

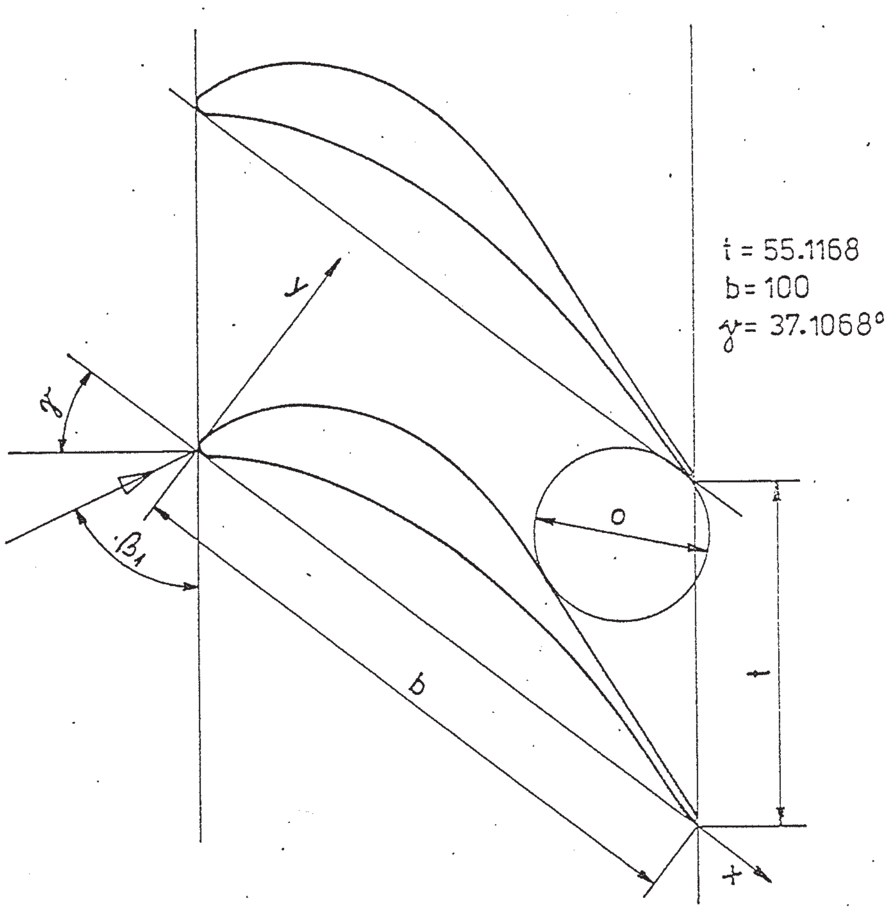

Fig. 2 The scheme of the SE1050 turbine blade cascade

4. The Optical Measurement Results

The interferograms in Fig. 3 present the flow development from subsonic to supersonic exit velocities in the blade cascade. The interferometer was set for infinite interference fringe. The subsonic blade cascade flow is presented in Figs. 3a, 3b, 3c. A stronger adverse pressure gradient downstream of the maximum velocity on the suction side indicates that the cascade was designed most likely for transonic velocities. Boundary layer transition occurs in the middle of the suction side. By comparing all three pictures one can prove the similarity of the compressibility effect known as the Prandtl-Glauert rule or the more general Karman-Tsien rule. Fig. 3d presents a transonic regime. The local supersonic region on the suction side is terminated by an almost normal shock wave located still inside the channel. Downstream of the shock a boundary layer transition to turbulence follows. The interferometric method (Figs. 3c and 3d) enabled us to evaluate the critical isentropic exit Mach number 0.748 in the SE 1050 turbine blade cascade. The periodical wakes are relatively wide, kinetic energy loss coefficient should be higher. Typical transonic regimes at aerodynamic choking are presented in Figs. 3e, 3f. The sonic line crosses the inter-blade channel. The subsonic flow upstream of the cascade should not be influenced by the pressure downstream of the cascade. The local supersonic region is terminated by a shock wave. Then the flow is accelerated into supersonic velocities at the trailing edge and decelerated into subsonic velocities by the external branch of the exit shock waves. In Fig. 3e a development of a vortex street in the wake appears although the trailing edge was modified to achieve a small effective thickness. Kinetic energy loss coefficient will be higher. At the regime shown in Fig. 3f, the vortex street disappears, the wake is relatively thin. In Figs. 3g, 3h, 3i, 3j regimes with supersonic exit are presented. In Fig. 3g the inner branch of the exit shock waves terminates the intensive supersonic expansion at the beginning of the cascade exit. The shock reflects on the suction side of the neighbour profile as the Mach reflection structure. In Fig. 3h the shock wave reflection is formed as a regular structure. The wakes downstream of the trailing edges are thin. Approximately at the half chord of the suction side a curious effect occurs. We call this effect "supersonic compression accompanying transonic expansion". The compression is a consequence of the discontinuity of curvature of the suction side surface at the point of velocity decrease. We fully understand this effect and we are able to control it by the suction side shape. We have investigated [2] the influence of the local supersonic compression on the boundary layer development. Our experience is that numerical methods that do not solve the above mentioned flow effects have to be revised. In Figs. 3i, 3j higher supersonic velocities at the cascade exit are shown. The flow field structure is similar to the previous regime, but the wakes apparently deviate to higher exit angles. This effect is called supersonic flow deviation at the exit part of the blade cascade. In the regime shown in Fig. 3j the limit load is exceeded. It can be recognized by the position of the inner branches of the exit shock waves. They do not reflect from the suction side of the neighbour blade. They pass its trailing edge and consequently pass the trailing edges of all next blades. Optical methods help us to detect a very serious experimental problem - the occurrence of parasite tunnel wave. It can be observed in Fig. 3j downstream of the blade cascade.

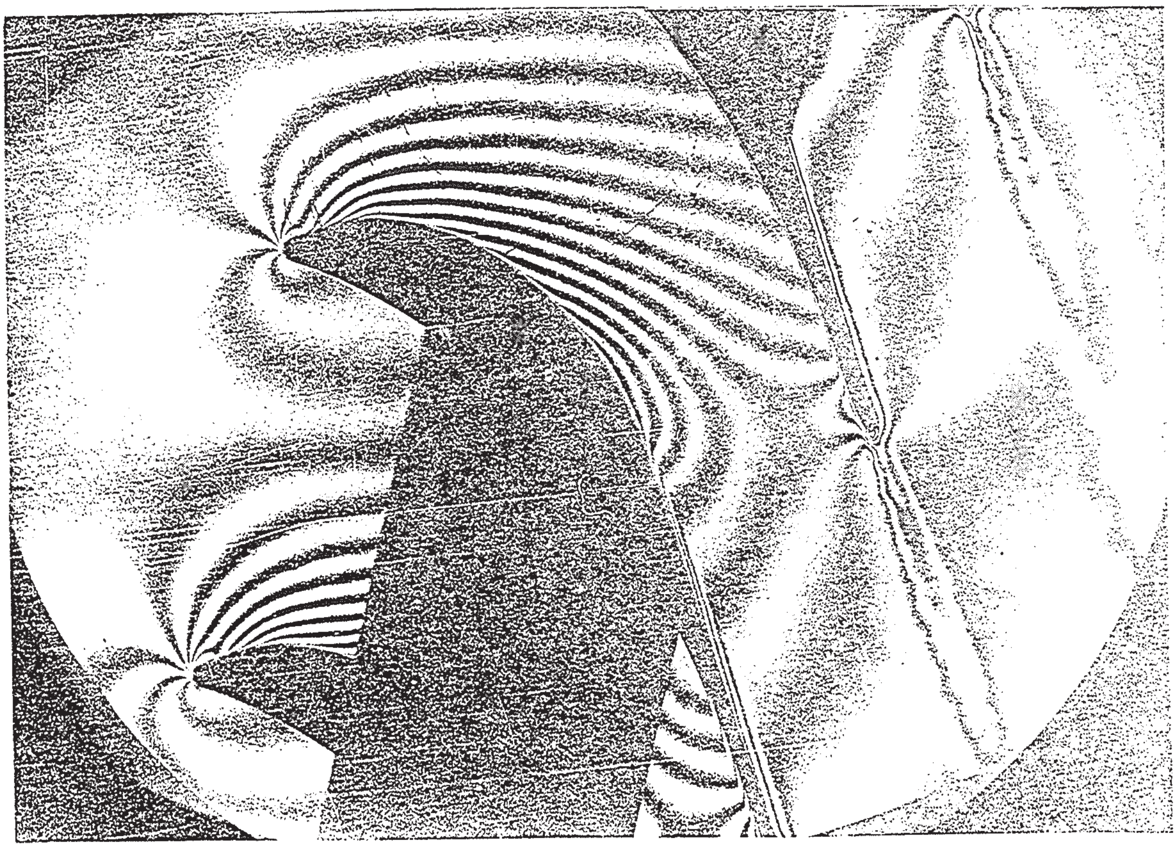

a. $M_1 = 0.279$, $\beta_1 = 70.7°$, $M_{2is} = 0.489$

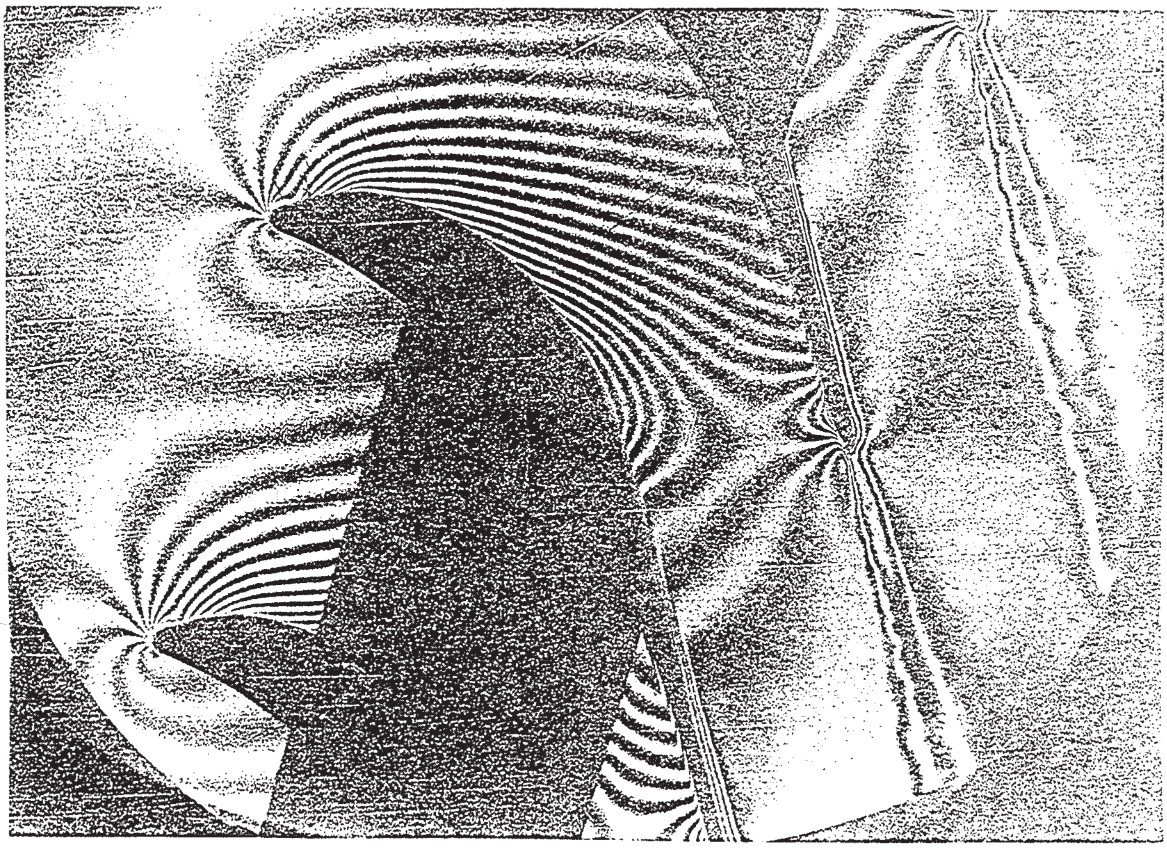

b. $M_1 = 0.322$, $\beta_1 = 70.7°$, $M_{2is} = 0.610$

Fig. 3 Interferograms of the flow in the SE1050 turbine blade cascade

c. M_1 = 0.354, β_1 = 70.7°, M_{2is} = 0.716

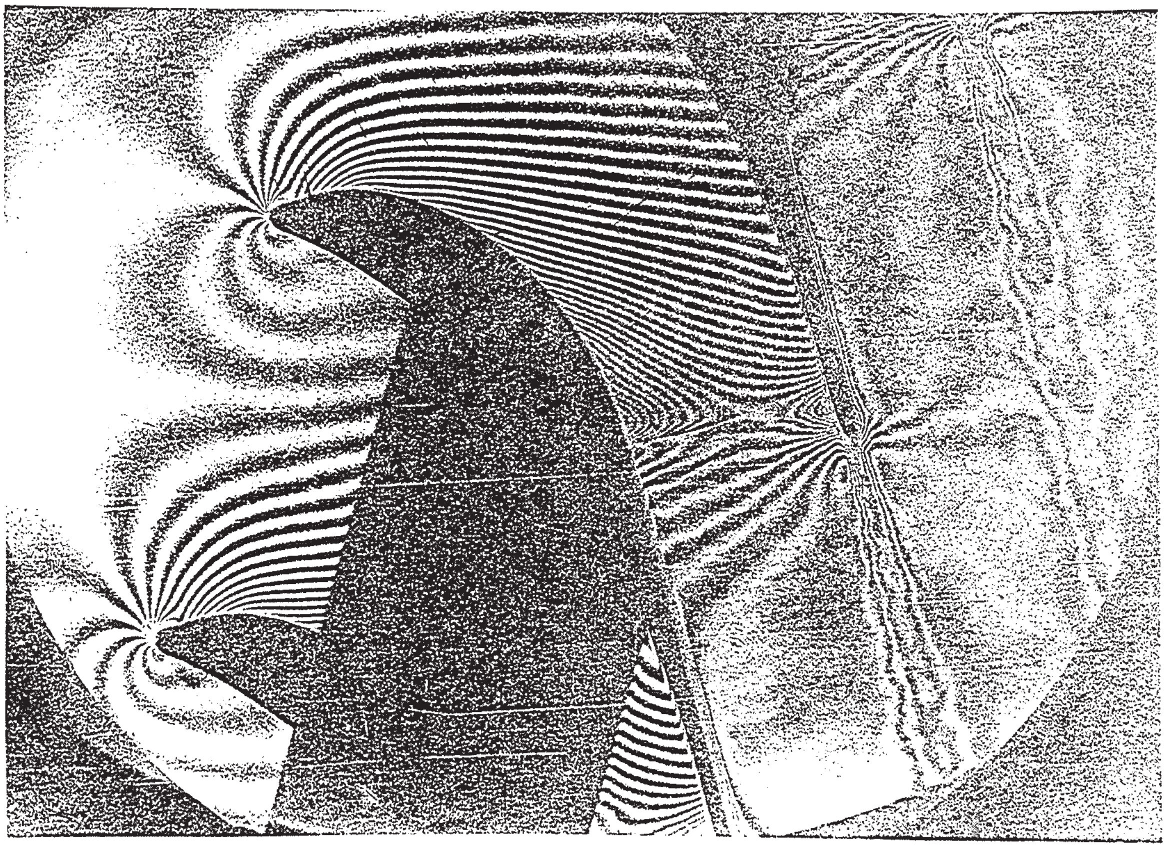

d. M_1 = 0.364, β_1 = 70.7°, M_{2is} = 0.793

Fig. 3 Interferograms of the flow in the SE1050 turbine blade cascade (continued)

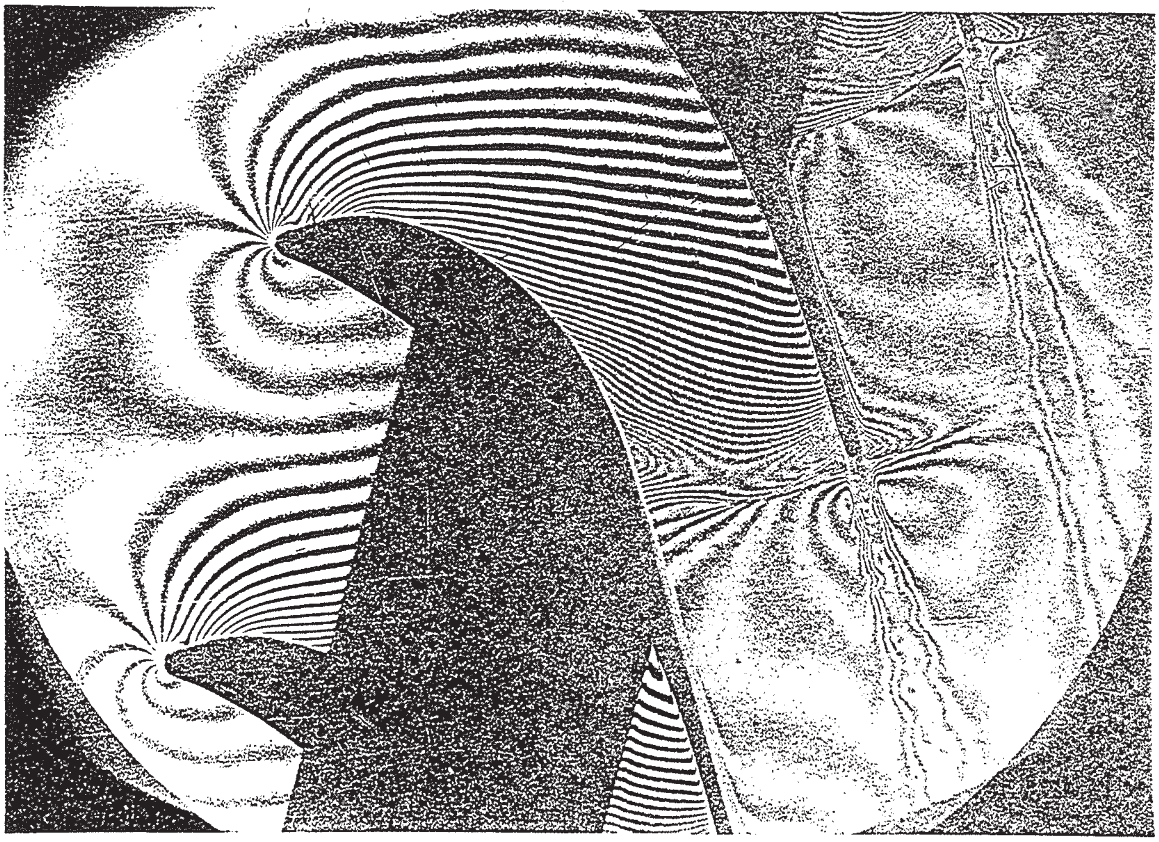

e. $M_1 = 0.365$, $\beta_1 = 70.7°$, $M_{2is} = 0.906$

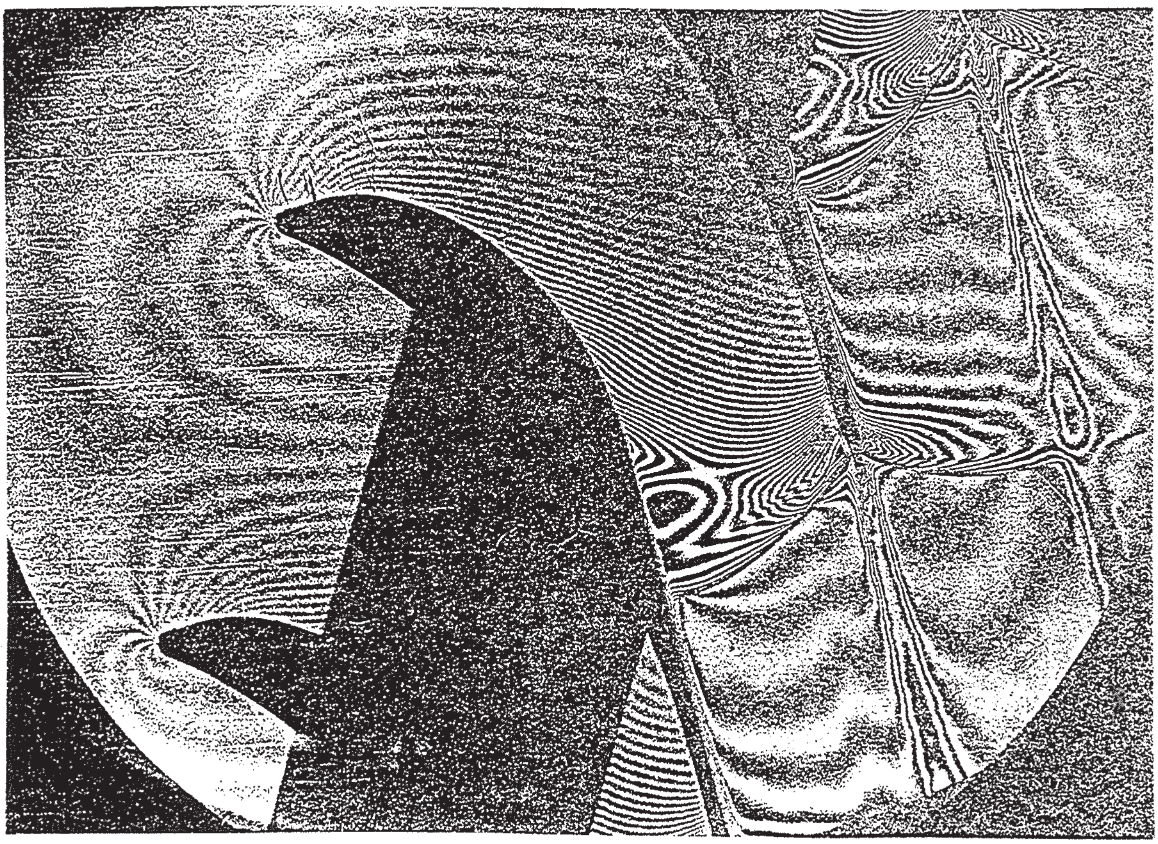

f. $M_1 = 0.371$, $\beta_1 = 70.7°$, $M_{2is} = 1.007$

Fig. 3 Interferograms of the flow in the SE1050 turbine blade cascade (continued)

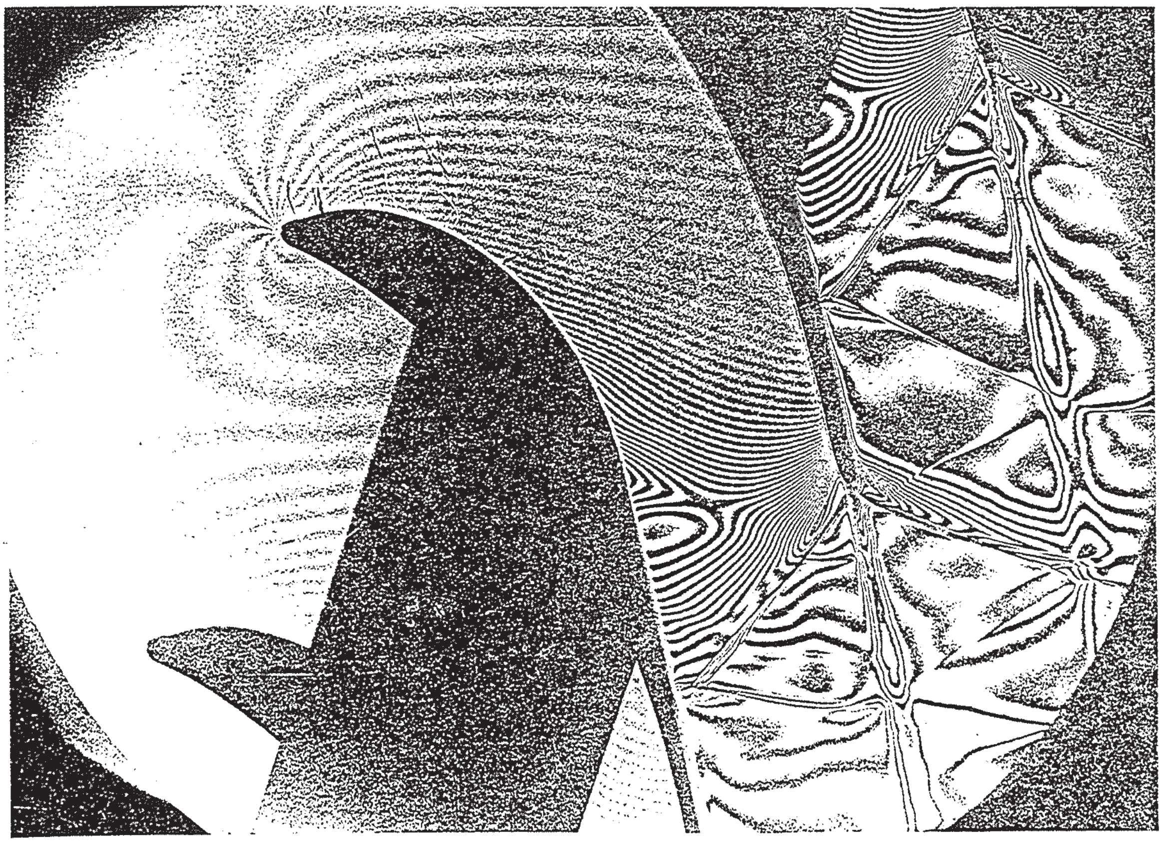

g. $M_1 = 0.376$, $\beta_1 = 70.7°$, $M_{2is} = 1.099$

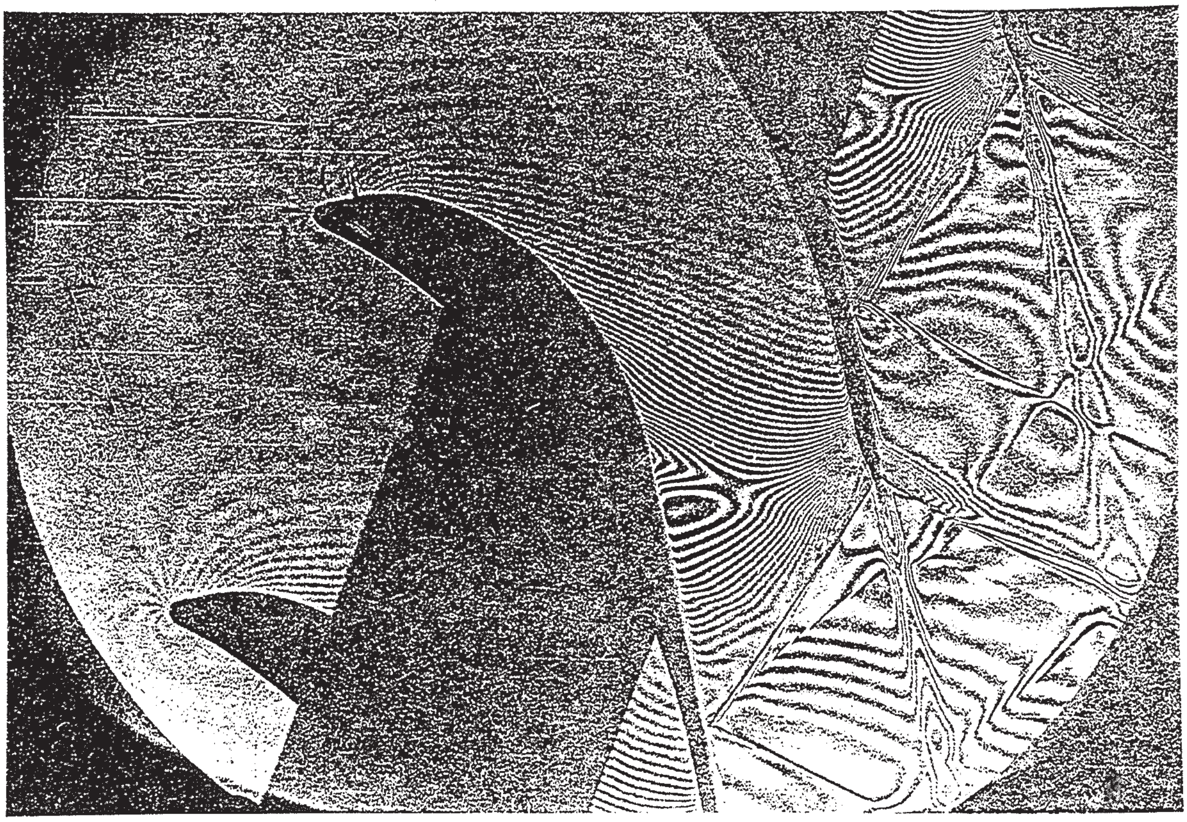

h. $M_1 = 0.375$, $\beta_1 = 70.7°$, $M_{2is} = 1.198$

Fig. 3 Interferograms of the flow in the SE1050 turbine blade cascade (continued)

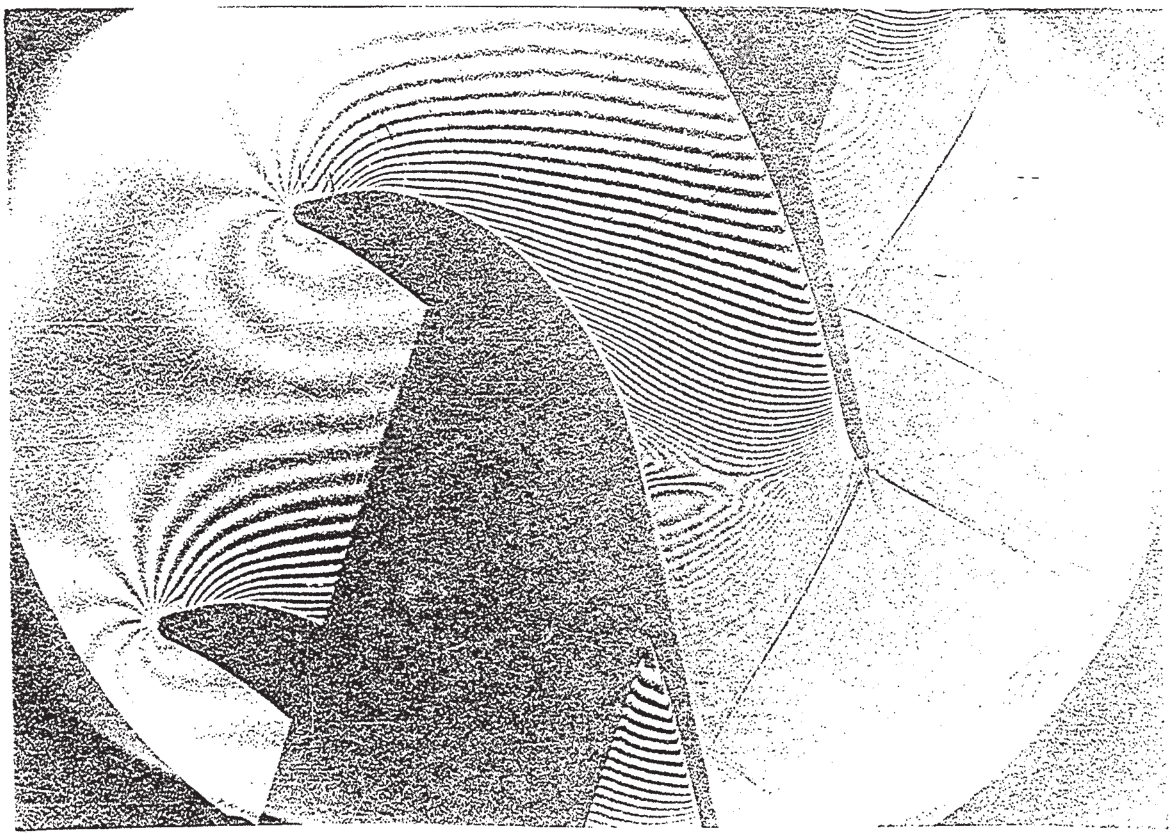

i. $M_1 = 0.379$, $\beta_1 = 70.7°$, $M_{2is} = 1.313$

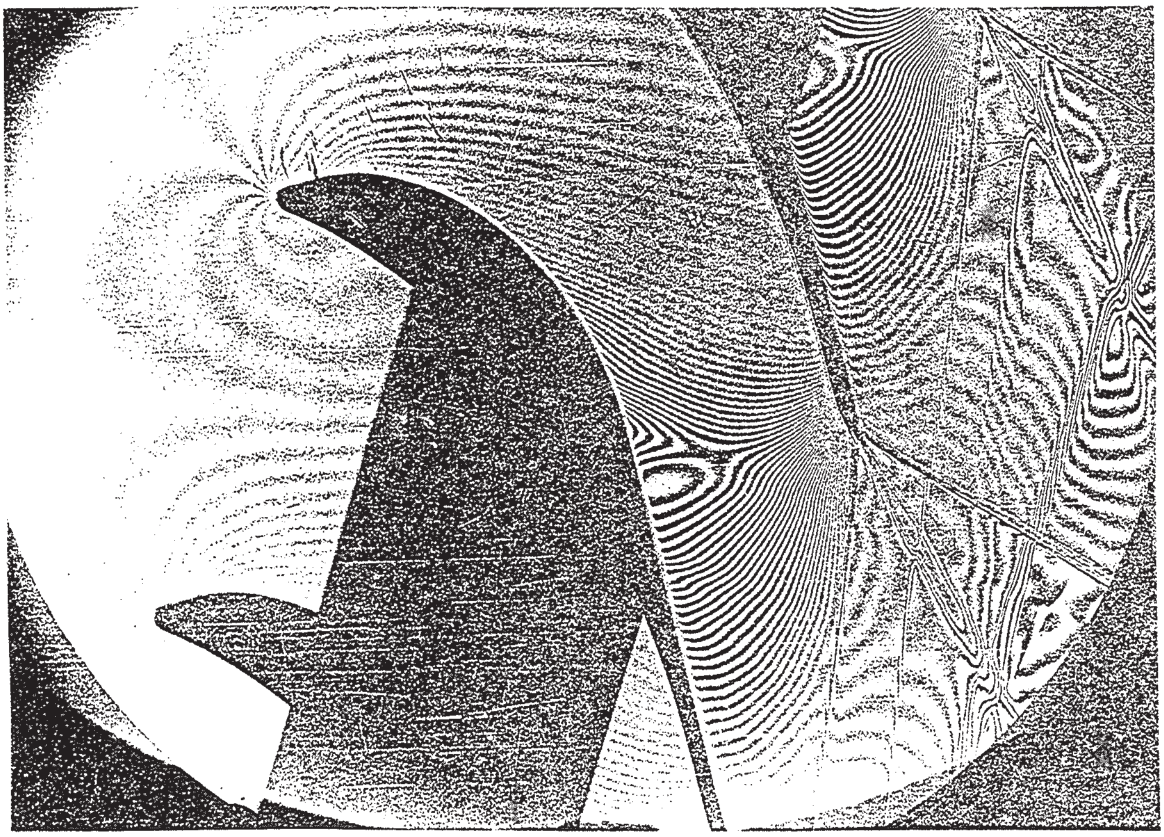

j. $M_1 = 0.377$, $\beta_1 = 70.7°$, $M_{2is} = 1.387$

Fig. 3 Interferograms of the flow in the SE1050 turbine blade cascade (continued)

5. Evaluation of Interferograms

The procedure of evaluating interferograms with infinite interference fringe is not difficult. It consists of numbering fringes, solving the local flow medium density and recalculating other parameters under assumption of isentropic flow. Although numbering of fringes follows simple rules, it should be performed by an experienced person. More complicated situation happens during numbering through shock waves. Nevertheless, an experienced and careful assistant can deal with problems successfully. Solution of local flow medium density value carries out according to the equation

$$(\rho)_i = (\rho)_0 - C \cdot i \,. \tag{1}$$

$(\rho)_i$ is flow density for the i-th fringe, $(\rho)_0$ is flow density for the zero-th fringe whose parameters are measured independently. i is the number of the fringe where the positive value corresponds to flow acceleration, i.e. density decrease. C is the constant of our interferometric system

$$C = \frac{\lambda}{K \cdot L} = 0.011858 \ \mathrm{kg \cdot m^{-3}} \,. \tag{2}$$

The value of the constant is very convenient. It represents approximately 100 interference fringes in the region from barometric density to vacuum. λ is wave length $\lambda = 4.358 \cdot 10^{-7}$ m. Blue monochromatic light close to violet is used. L is wind tunnel width L = 0.16 m, and K is the Gladstone-Dale constant; $K = 2.297 \cdot 10^{-4} \ \mathrm{kg \cdot m^{-3}}$ for air. Isentropic flow parameters are solved according to the relations:
for pressure

$$p_{is} = p_0 \cdot \left(\frac{\rho}{\rho_0} \right)^{\kappa} \tag{3}$$

for non-dimensional velocity

$$\lambda_{is} = \sqrt{\frac{\kappa + 1}{\kappa - 1} \cdot \left[1 - \left(\frac{\rho}{\rho_0} \right)^{\kappa - 1} \right]} \,. \tag{4}$$

p_0 and ρ_0 are total pressure and total density, respectively. κ is ratio of heat capacities, κ = 1.4 for air. An error analysis proved that the application of the interferometric method is very convenient for transonic measurements.

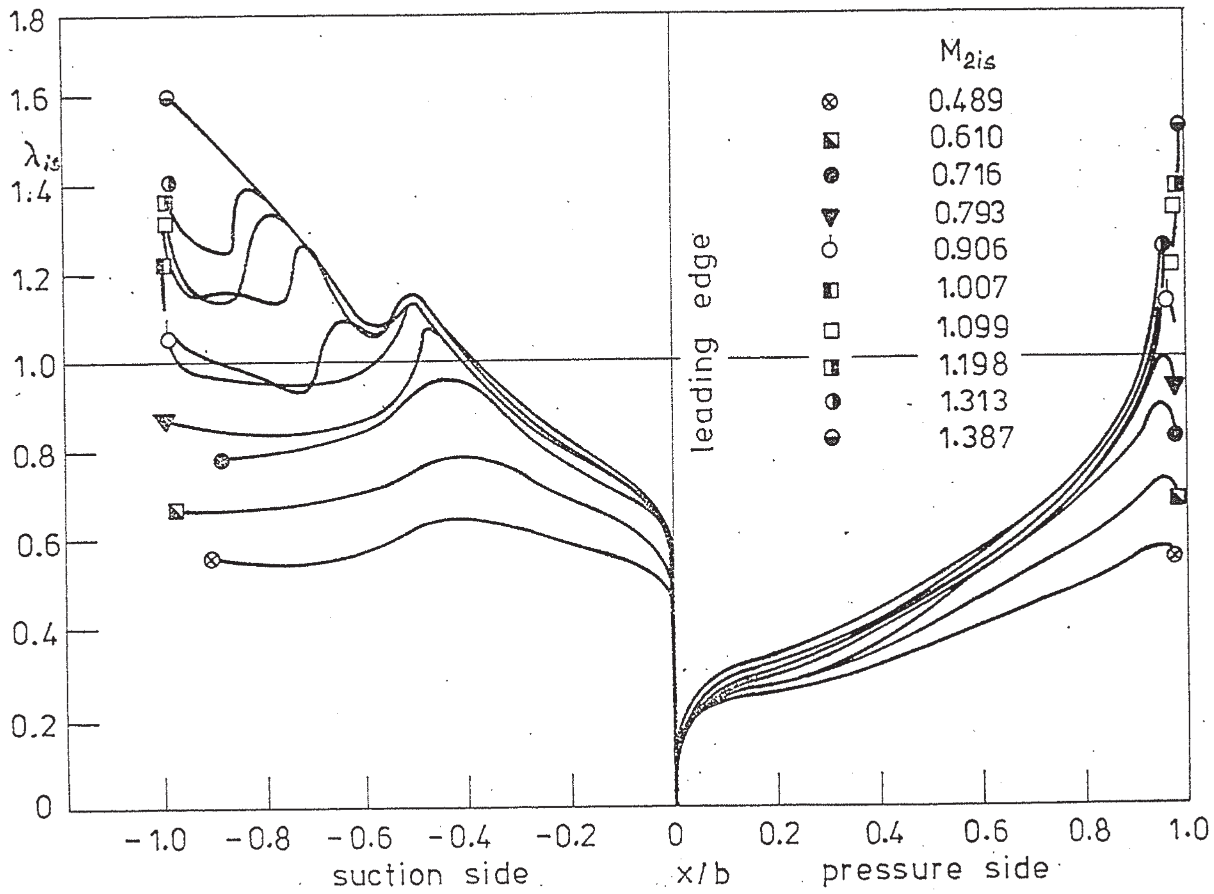

Fig. 4 Distribution of the relative velocity along the profile SE1050

6. Results of Evaluations

The described evaluation method has been applied for evaluating the series of all interferograms shown in Sec. 4. The result of distribution of isentropic non-dimensional velocity on the profile surface is presented in Fig. 4. From the diagram it is possible to recognize three subsonic regimes, three typical transonic regimes and four regimes with supersonic exit velocities. The local velocity decrease at the half of suction side for the four supersonic cases and one transonic case is caused by the above mentioned effect of supersonic compression accompanying transonic expansion.

7. The Extreme Incidence Measurements

The leading edge separation occurs when the incidence angles of flow past the blade cascade are extremely large. In the interferogram in Fig. 5 the case of extreme part load mode of operation is shown. The leading edge separation occurs on the pressure side and the flow again reattaches to the pressure side. Interferometric method indicates explicitly the point of the reattachment. In Fig. 5 the reattachment is near the local density maximum on the pressure side at about 60% chord length.

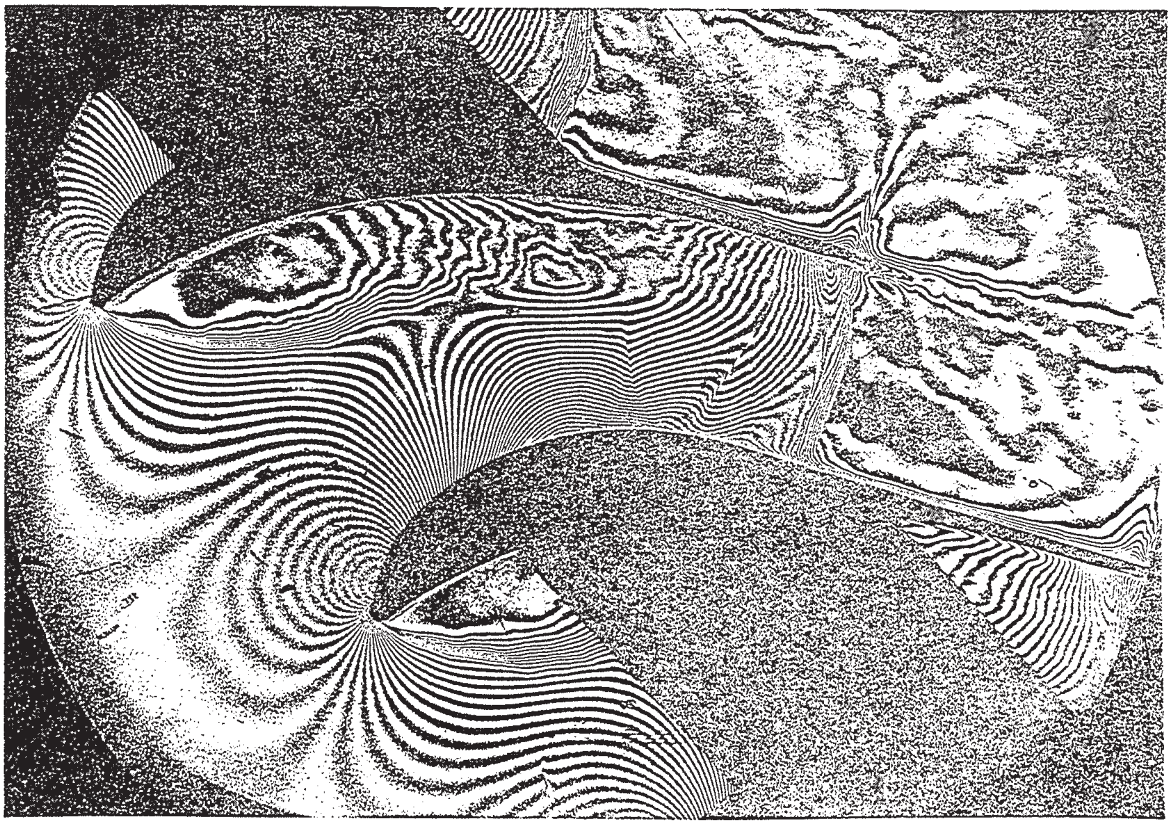

Fig. 5 Interferogram of the flow in the SE 1050 blade cascade
(i = - 67°, M_{2is} = 0.905)

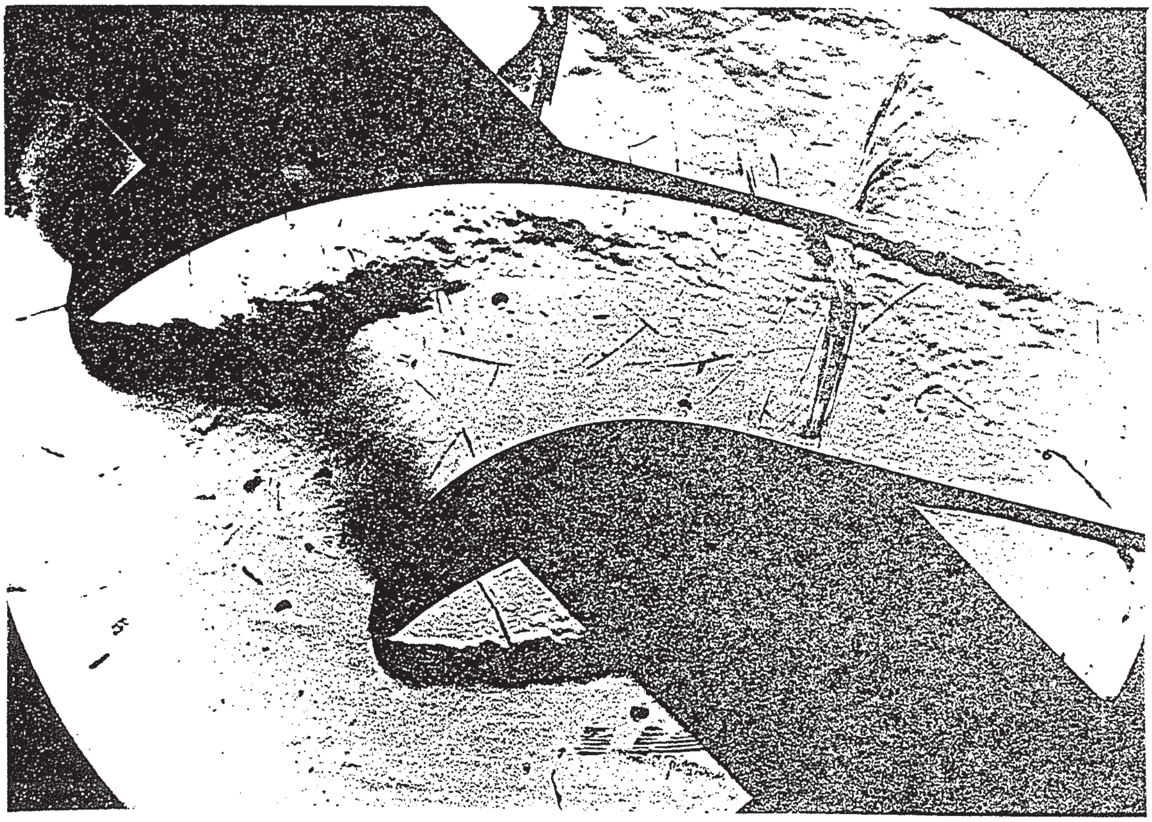

Fig. 6 The schlieren picture of the flow in the SE 1050 blade cascade
(i = - 67°, M_{2is} = 0.905)

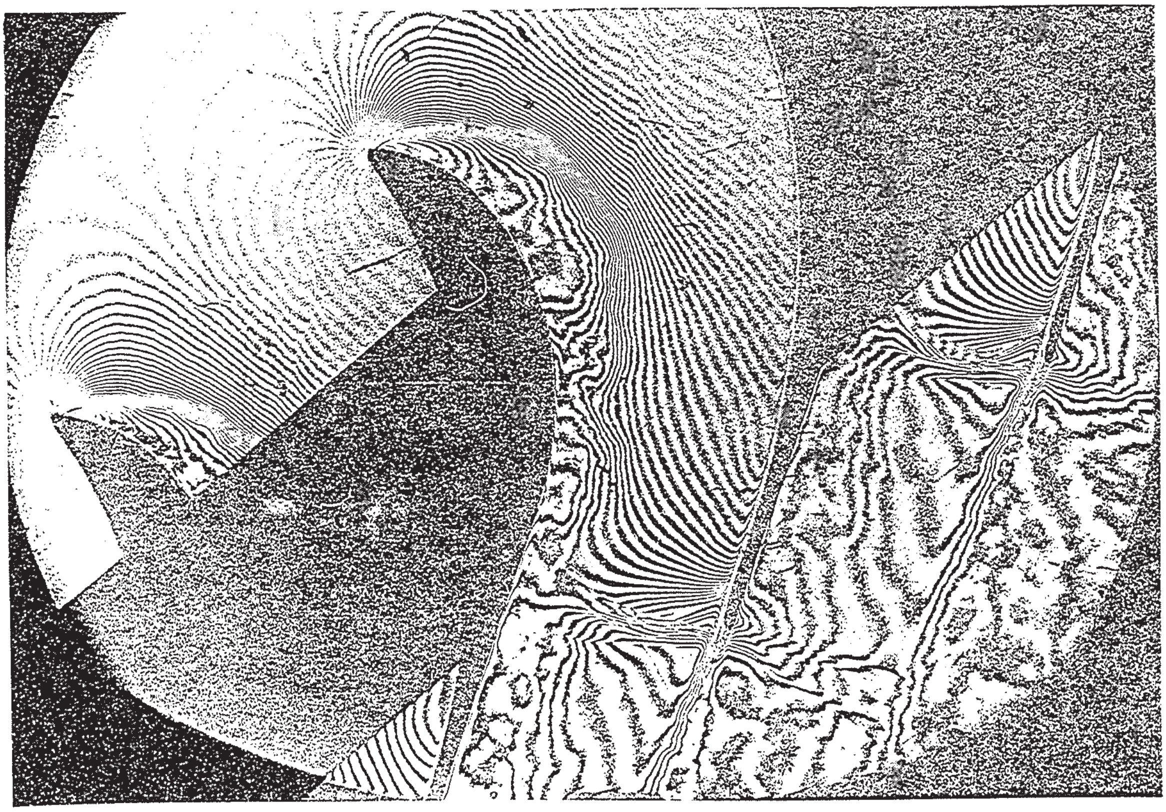

Fig. 7 Interferogram of flow in the SE 1050 blade cascade
(i = + 30°, M_{2is} = 1.012)

Other transonic flow structures can be observed in the interferogram in Fig. 5. The schlieren picture in Fig. 6 was taken at the same regime as the interferogram in Fig. 5. In the schlieren picture we can observe a rough structure in the separation region along the whole pressure side and along the wake downstream of the cascade. The rough structure is due to turbulence in the flow field. The potential core of the flow is represented by the smooth area upstream of the cascade, and along suction side up to the shock wave terminating the local supersonic region. The interferogram in Fig. 7 represents transonic flow field at extreme incidence for the overload regime. The leading edge separation on the suction side has a wavy character. Apparently the reattachment of the flow on the suction side in the region 30 to 40 % chord is not steady.

8. Conclusions

Optical research techniques enable us to obtain an insight into real transonic blade cascade flow fields. Their applications at high-speed aerodynamic tests have proved to be a powerful tool for investigations. The development of the blade cascade flow is presented in the series of interferograms. The interferograms were evaluated, and analysed. The interferograms and the schlieren picture from extreme incidence measurements are compared.

9. References

[1] Šťastný M., Šafařík P. : *Experimental Analysis Data on the Transonic Flow Past a Plane Turbine Cascade*, ASME Paper No.90-GT-313

[2] Šťastný M., Šafařík P. : *Boundary Layer Effects on the Transonic Flow in a Straight Turbine Cascade*, ASME Paper No.92-GT-155

Acknowledgements

The research was carried out in co-operation of ŠKODA, Turbines, Plzeň with the Czech Technical University, Faculty of Mechanical Engineering, Prague. The optical measurement system was installed and used in the Institute of Thermomechanics, Academy of Sciences of the Czech Republic.